Energy and momentum transfer in one-dimensional trapped gases by stimulated light scattering

2015 New J. Phys. 17 063012

(http://iopscience.iop.org/1367-2630/17/6/063012)

IOP Publishing New J. Phys. 17 (2015) 063012 doi:10.1088/1367-2630/17/6/063012

New Journal of Physics
The open access journal at the forefront of physics

Deutsche Physikalische Gesellschaft DPG
IOP Institute of Physics

Published in partnership with: Deutsche Physikalische Gesellschaft and the Institute of Physics

OPEN ACCESS

RECEIVED
5 February 2015

REVISED
16 April 2015

ACCEPTED FOR PUBLICATION
1 May 2015

PUBLISHED
10 June 2015

PAPER

Energy and momentum transfer in one-dimensional trapped gases by stimulated light scattering

N Fabbri[1,2], C Fort[1,2], M Modugno[3,4], S Rosi[1,2] and M Inguscio[1,5]

[1] LENS European Laboratory for Non-linear Spectroscopy, and Dipartimento di Fisica e Astronomia-Università di Firenze, I-50019 Sesto Fiorentino, Italy
[2] CNR-INO Istituto Nazionale di Ottica, I-50019 Sesto Fiorentino, Italy
[3] Dpto. de Física Teórica e Historia de la Ciencia, Universidad del País Vasco UPV/EHU, 48080 Bilbao, Spain
[4] IKERBASQUE, Basque Foundation for Science, 48011 Bilbao, Spain
[5] INRIM Istituto Nazionale di Ricerca Metrologica, I-10135 Torino, Italy

E-mail: fabbri@lens.unifi.it

Keywords: quantum gases, bragg spectroscopy, 1D bosons

Abstract

In ultracold atoms settings, inelastic light scattering is a preeminent technique to reveal static and dynamic properties at nonzero momentum. In this work, we investigate an array of one-dimensional trapped Bose gases, by measuring both the energy and the momentum imparted to the system via light scattering experiments. The measurements are performed in the weak perturbation regime, where these two quantities—the energy and momentum transferred—are expected to be related to the dynamic structure factor of the system. We discuss this relation, with special attention to the role of in-trap dynamics on the transferred momentum.

1. Introduction

Stimulated scattering of light or particles from condensed-matter systems—solids, liquids, and gases—is a powerful tool for providing fundamental insight into the structure of matter. Elastic scattering of x-ray photons has permitted to disclose the atomic order and electron distribution in crystalline solids, as well as the arrangement of atoms in molecules [1]. Similarly, inelastic neutron scattering has unveiled the phonon spectrum of superconductors and the superfluidity of liquid helium [2].

In cold atomic systems, inelastic scattering of photons–also known as Bragg spectroscopy–has been used to study Bose–Einstein condensates (BECs) in harmonic three-dimensional (3D) traps [3–5], quasi-condensates in a quasi one-dimensional (1D) trap [6], BECs in shallow cubic optical lattices [7, 8], strongly interacting BECs across a Feshbach resonance [9], and strongly interacting fermions [10, 11], through direct observation of the net momentum imparted to the system. The transferred momentum is easily measured in this kind of settings, since the atomic density distribution, observed after time-of-flight in the far-field regime, directly reflects the in-trap momentum distribution.

Strongly correlated phases of bosons in optical lattices have been investigated by measuring the increase of energy following the external perturbation. The quantum phase transition from a superfluid to a Mott-insulator state has been studied in 1D Bose gases in the presence of a longitudinal lattice with experiments of lattice amplitude modulation, where the excitation has zero momentum [12], and with scattering experiments where the excitation has non-zero momentum [13, 14]. The latter technique has been also used for studying 1D gases in optical lattices [15, 16]. The energy of a condensate, even in the presence of shallow lattices, is easily extracted from the time-of-flight density distribution of the gas [17], whereas the energy of strongly-interacting systems realized in deep optical lattices–as a Mott insulator–is not directly accessible, unless with single-site resolution experiments [18]. In the case of deep optical lattices, the energy excess produced by the Bragg perturbation can be measured by lowering the lattice depth, i.e., driving the system in a less interacting regime, and letting it thermalize [12, 13].

In the linear response regime, both energy and momentum transfer are related to the dynamic structure factor [19], which carries key information about the dynamical behaviour and correlations of the system. However in trapped condensates, while the energy is a conserved quantity, momentum is not conserved due to the presence of the trap. Thus, if the Bragg pulse duration is not negligible compared to the inverse of the trap frequency, the momentum imparted by the Bragg beams can be affected by the in-trap dynamics [19, 20], complicating its connection to the dynamical structure factor. On the other hand, a short Bragg pulse would result in a limited spectral resolution.

In this work, we use inelastic light scattering for accessing the dynamic structure factor of an array of 1D Bose gases. The dimensionality of the system plays a crucial role: in 1D quantum systems, correlations—which directly reflect on the dynamic structure factor—lead to peculiar phenomena, such as fermionization of strongly-interacting bosons [21–23], or spin-charge separation of interacting fermions [24], which do not have any higher-dimensional equivalent. Moreover, for 1D systems, the mechanisms and characteristic times of thermalization are currently under investigation [25, 26]. This may affect the measurement of the energy transferred via light scattering. On the other side, momentum measurement of 1D trapped gases may be influenced by the in-trap dynamics, as above mentioned. The purpose of this work is to investigate experimentally the relation between energy and momentum imparted to an array of 1D gases due to Bragg scattering, in a typical regime of parameters [13, 16], and to discuss the effect of the in-trap dynamics on the transferred momentum.

The paper is organized as follows. In section 2 we focus on the comparison of the response of the array of 1D gases to the scattering experiments in terms of energy deposited and momentum boost imparted to the system. We present the experimental setup and discuss the results, obtained in a regime of weak perturbation. We also directly compare the susceptibility of this system to the one of a 3D non-interacting condensate. In section 3 we study the effect of the in-trap dynamics on the momentum transfer by recording the evolution of the response of the system in time, after the Bragg excitation.

2. Energy and momentum transferred to an array of 1D gases

2.1. Experimental setup

We produce an array of 1D gases by loading a Bose–Einstein condensate of about 2.5×10^5 ^{87}Rb atoms in a two-dimensional optical lattice created by two mutually orthogonal standing laser waves of wavelength $\lambda = 765$ nm. The loading is performed with an exponential ramp of $t_r = 250$ ms, with time constant $t_r/3$. The final depth of the lattice is $V_L = 30E_r$, with $E_r = h^2/(2m\lambda^2)$, m being the atomic mass and λ the lattice wavelength. This value is chosen to be high enough to freeze the transverse degrees of freedom of each 1D gas (the radial trapping frequency is $\omega_\perp = 2\pi \times (42 \pm 2)$ kHz), and suppress the tunneling of particles between different tubes on the timescale of the experiment.

The equilibrium state of the system is completely described by two dimensionless parameters [27], that is, (i) the interaction parameter $\gamma = mg_{1D}/(h^2\rho)$, where g_{1D} is the 1D interaction strength [29] and ρ the density, and (ii) the reduced temperature $\tau = 2mk_BT/(\hbar\rho)^2$, which depends on both density ρ and temperature T. In this work, we explore a regime of $\gamma \simeq 1$ and $\tau \simeq 1$.

The significant parameters that characterize the 1D gases vary overall the array. Their distribution can be estimated by rescaling the interparticle interaction strength g_{3D} as in [16], given the overall trapping frequencies in the presence of the lattices, $\omega_x = 2\pi\,(63 \pm 13)$ Hz, $\omega_y = 2\pi\,(60 \pm 10)$ Hz, $\omega_z = 2\pi\,(76 \pm 15)$ Hz. We estimate the array to consist of about 4×10^3 1D tubes, and the central tube to have $\gamma = (0.9 \pm 0.2)$, density $\rho = (5 \pm 1)\,\mu\text{m}^{-1}$, and chemical potential $\mu/h = (3.9 \pm 0.7)$ kHz. The average values of these parameters—obtained weighting the contribution of each tube of the array with its number of atoms—are $\overline{\gamma} = (1.4 \pm 0.4)$, $\overline{\rho} = (3.7 \pm 0.8)\,\mu\text{m}^{-1}$, and $\overline{\mu}/h = (3.6 \pm 0.6)$ kHz.

The study of this system is carried out by imparting a perturbation to the array of 1D tubes given by two simultaneous off-resonance laser pulses with time duration $t_B = 3$ ms, which determines an interaction-time broadening of $\simeq$150 Hz. Note that $t_B \simeq T/5$, with $T = 2\pi/\omega_x$ being the trap period along the axis of the tubes. The laser light is detuned by 200 GHz from the ^{87}Rb resonance and the waist of the Bragg beams is $\simeq 900\,\mu$m. The two beams have tunable relative detuning $\Delta\omega$ (up to tens of kHz), and produce a moving Bragg grating with amplitude $V_B = h \times 900$ Hz. The wavevector of the Bragg grating is adjusted to be along the axial direction of the tubes, and it is fixed at $q = (7.3 \pm 0.2)\,\mu\text{m}^{-1}$. Comparing the Bragg wavevector with the average value of the healing length ξ [30], we have $q\xi \simeq 0.9$. Since in our case the healing length is about a half of the interparticle distance, the mean-field picture does not apply, and a more convenient length scale is given by the inverse of the Fermi wavevector, which in our case is $k_F = \pi\rho \simeq 2q$. In the experiments, we vary the energy $\hbar\omega$ of the excitation by tuning $\Delta\omega$ (being $\omega = |\Delta\omega|$) and we measure the response of the system, in terms of energy and momentum transfer.

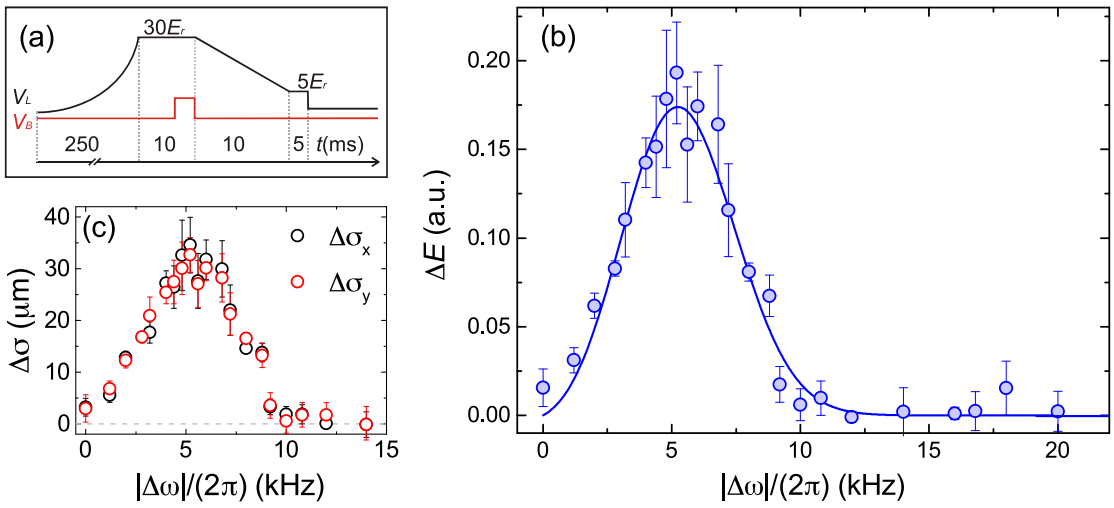

Figure 1. Energy transfer. (a) Experimental timing used for measuring the energy spectrum. The optical lattice is raised to $30E_r$ in 250 ms. During the holding time the Bragg beams are shone onto the atoms, then the whole system is let thermalize by lowering the lattice depth to $5E_r$. After 5 ms the trap is released, and the energy is measured from the time-of-flight density distribution. (b) Energy transferred via Bragg scattering to an array of 1D gases in an optical lattice of height $V_L = 30\ E_r$, as a function of the excitation frequency. The signal is obtained from the squared width of the central peak of the time-of-flight density distribution $(\sigma_x^2 + 2\sigma_y^2)$. The fitting curve is given by a gaussian function multiplied by the frequency $\omega G(\omega)$. (c) Increase of the rms size along the axis of the tubes (σ_x) and along a perpendicular axis (σ_y), as a function of the excitation frequency.

2.2. Results

Here, we present the measurement of the energy transfer, which is a conserved quantity even in the presence of a trapping potential. For measuring the energy transfer, after the Bragg pulse we lower the lattice height to $V_L = 5E_r$, where the different lattice sites are coupled via tunneling of particles on a timescale of ~0.6 ms, and the temperatures of the different gases can re-equilibrate to a common value of the 3D system. After 5 ms the gas is released and let expand ballistically for a time-of-flight $t_{\rm tof} = 25$ ms, then we record the density distribution of the atomic cloud. The experimental timing, see also [13, 28], is sketched in the figure 1(a). From the time-of-flight images, we extract the squared width of the central peak of the resulting interferogram $\sigma^2 = \sigma_x^2 + 2\sigma_y^2$ [6] and subtract the background σ_0^2, corresponding to the value measured in the absence of the Bragg pulse, in order to obtain the experimental signal. This quantity is proportional to the energy imparted to the system, as previously demonstrated [16]. The latter, in turn, is related to the dynamic structure factor $S(q, \omega)$ of the system through the relation [31]

$$\Delta E(q, \omega) = \left(\frac{2\pi}{\hbar}\right)\left(\frac{V_B}{2}\right)^2 t_B\, \omega S(q, \omega), \tag{1}$$

valid in the linear response regime. The measured energy spectrum, normalized to its integral, is shown in figure 1(b). In order to verify that the system has thermalized after the Bragg pulse, in figure 1(c) we plot separately the increase of the rms size observed in each direction ($\Delta\sigma_x$ and $\Delta\sigma_y$): in spite of the symmetry breaking induced by the Bragg perturbation imparted along the axis of the 1D gases (x direction), $\Delta\sigma_x$ and $\Delta\sigma_y$ show the same dependence on the Bragg frequency, indicating that an efficient thermalization process has occurred during the ramping down of the lattices.

In the experiment, we also measure the total momentum imparted to the same system. To this purpose, after the Bragg pulse, the atoms are abruptly released directly from the trap, as represented in figure 2(a), so that in-trap momentum is mapped into the atomic density distribution after time-of-flight. When the Bragg perturbation is on resonance, momentum is transferred efficiently, and the time-of-flight images of the density distribution exhibit a small cloud of excited atoms ejected from the main cloud. Figure 2(b) shows the evolution of the normalized density profiles $n(x)$ integrated along the line of sight and along the y direction (orthogonal to the axis along which momentum is transferred) with the relative detuning between the Bragg beams. From the time-of-flight images, the net moment boost $\Delta P(\omega, q)$ is obtained by measuring the displacement of the center of mass—relative to the unperturbed position—as [32]

[6] Here, we have assumed $\sigma_y = \sigma_z$ owing to the cylindrical symmetry of the system.

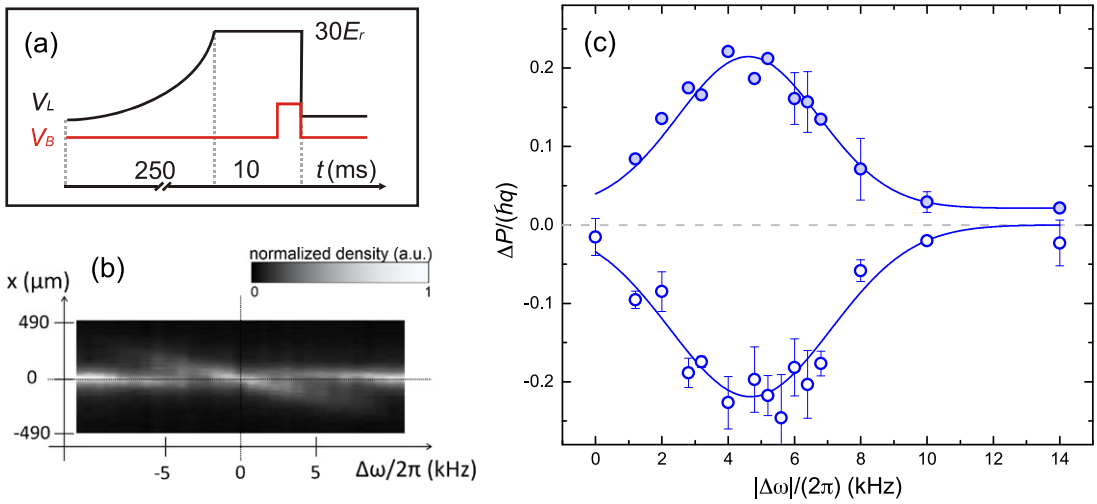

Figure 2. Momentum transfer. (a) Experimental timing. The optical lattices are abruptly switched off immediately after the Bragg pulse, and the momentum transfer is measured from the center-of-mass shift of the whole cloud. (b) Normalized density profile $n(x)$ along the axis of the 1D gases—integrated along the line of sight z and the y direction—for different values of the relative detuning of the Bragg beams $\Delta\omega/(2\pi)$ (false colours). On resonance, the central peak is depleted and the atoms are ejected along the x direction. (c) Momentum transferred to an array of 1D gases. The filled (empty) dots, at positive (negative) momentum along the axis of the tubes, correspond to $\Delta\omega < 0$ ($\Delta\omega > 0$). The Bragg parameters of this measurement are the same as described for the measurement of the energy transfer.

$$\Delta P(q,\omega) = \frac{m}{t_{\rm tof}} \int x\ (n(x,y) - n_0(x,y))\ {\rm d}x{\rm d}y, \tag{2}$$

where $n(x, y)$ and $n_0(x, y)$ are the density profiles integrated along the line of sight and normalized to the unity, with and without the Bragg excitation, respectively. The experimental spectra normalized to the momentum of the excitation $\hbar q$, $\Delta P(q, \omega)/(\hbar q)$, are shown in figure 2(c). Filled (empty) dots correspond to positive (negative) momentum, along the axis of the tubes.

As remarked in [19, 20, 33], momentum is a conserved quantity only in the absence of any external trapping potential. In this case, for a perturbation in the linear response regime and with $\omega t_B \gg 1$, $\Delta P(q, \omega)$ is related to the dynamic structure factor through the following relation

$$\Delta P(q,\omega) = \left(\frac{2\pi}{\hbar}\right)\left(\frac{V_B}{2}\right)^2 t_B\, qS(q,\omega). \tag{3}$$

For a trapped gas with axial trapping frequency ω_x significantly smaller than the radial one, this equation still holds in a wide range of parameters, provided that $\omega t_B \gg 1$ and $\omega_x t_B \ll 1$ [33]. In the present case, the first condition is well satisfied as $\omega t_B \simeq 80$ on resonance, while we have $\omega_x t_B \simeq 1$, which does not satisfy the second condition. Thus the comparison between the quantities extracted from the measurements of energy and momentum transfer is not straightforward. In order to address quantitatively this issue, we fit $\Delta P(q, \omega)$ with a gaussian function $G(\omega)$, where center, width and amplitude are free parameters, and $\Delta E(q, \omega)$ with $\omega\ G(\omega)$, as follows from equation 1. The gaussian centers obtained from the measured spectra are respectively (4.5 ± 0.2) kHz for the momentum transfer, and (4.3 ± 0.3) kHz for the energy transfer, with their widths being (2.5 ± 0.2) kHz and (2.3 ± 0.2) kHz, respectively. These results are consistent within the error bars, allowing us to conclude that, with this choice of parameters, both these experimental approaches measure the same quantity.

2.3. Comparison with the response of a 3D condensate

As a reference system, we also measured the transferred momentum of a 3D expanded condensate, since its response is well described by a non-interacting model. Before performing the scattering experiment, we switch off the trapping potential and let the BEC fall freely for 5 ms of time-of-flight, so that density decreases by a factor of ∼3, and the chemical potential drops to $\sim h \times 170$ Hz, hence the interparticle interactions can be neglected. For direct comparison, in figure 3 we show the experimental spectrum of the array of 1D gases obtained as previously described (figure 3(a)), and the spectrum of the 3D non interacting condensate (figure 3(b)). In both figures 3(a) and 3(b), the signal is normalized to the Bragg strength $V_B^2 t_B$. In this Figure, we also report the exact solution for a free-particle system (continuous red line), which shows an excellent agreement with the experimental data. This prediction is obtained by solving the Schrödinger equation [34] in the presence of the Bragg potential $V(x, t) = \theta(t - t_B) V_B \cos(qx - \omega t)$ (for $t \geqslant 0$), and does not contain any fitting parameter.

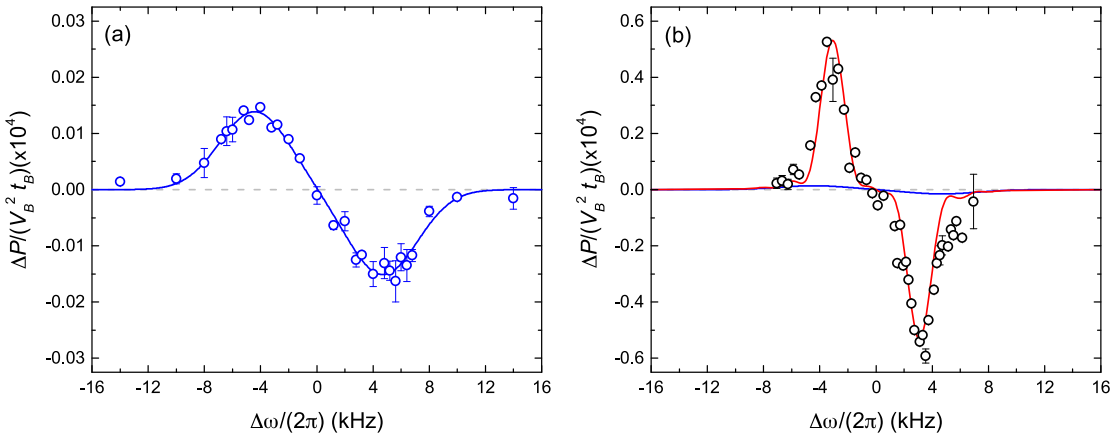

Figure 3. Comparison between the transferred momentum ΔP to (a) an array of trapped 1D gases and (b) a non-interacting 3D condensate. The horizontal scale represents the frequency difference between the Bragg beams. The spectrum of the array of 1D gases has been obtained using Bragg parameters $t_B = 3$ ms and $V_B = h \times 900$ Hz, whereas the spectrum of the 3D condensate has been obtained with $t_B = 0.5$ ms, and $V_B = h \times 540$ Hz. The amplitude of both the spectra has been rescaled by the pulse strength $V_B^2 t_B$ to directly compare the susceptibility of the two systems. Note that the vertical scale in the first graph is 20 times smaller than in the second one. A fit of the experimental spectrum of the 1D gases with a sum of two gaussian functions (blue curve) is shown in figure 3 (a) and reported also in figure 3 (b) for highlighting the comparison between the response of the two systems. The red continuous line in figure 3 (b) is the solution of the time-dependent Schrödinger equation for a non-interacting gas, given the value of V_B/h, with no free parameters (see text).

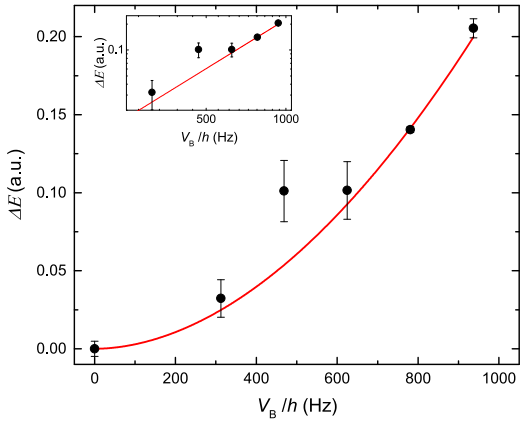

Figure 4. Test of the linear response regime. We report the energy increase of the array of 1D gases due to a resonant Bragg perturbation as a function of the amplitude of the Bragg grating, at fixed pulse duration $t_B = 3$ ms. The continuous red line is a power-law fit with free exponent m, resulting to be $m = (1.8 \pm 0.2)$, consistent with the quadratic behaviour expected in the linear response regime [19]. The inset shows the same data in log–log scale. The error bars are the standard deviations of up to ten repeated measurements.

From the comparison of the two spectra, we can notice that the response of the 1D tubes is much broader. A related work [16] shows that in the same regime of parameters the spectral broadening of the response of the array of 1D gases comes from the dynamics of the interaction-induced excitations.

Moreover, the comparison between the two amplitudes shows that the susceptibility of the 1D tubes is about 35 times lower than the one of the 3D non-interacting condensate. The very low susceptibility of the array of 1D tubes, with the Bragg parameters that we have used, is a first indication that the response of the system lies in a regime of weak perturbation, where the relations in equation (1) and equation (3) are expected to hold. We have also verified the behaviour of the experimental signal as a function of Bragg power in a range that includes the used value. This indicates the dependence of the signal on V_B to be quadratic (see figure 4), as expected in the framework of the linear response theory [19].

3. Effect of in-trap dynamics on the momentum transfer

As previously discussed, momentum is not a conserved quantity in the presence of a trapping potential. Therefore, the measurement of the momentum following a Bragg excitation can in principle be affected by the

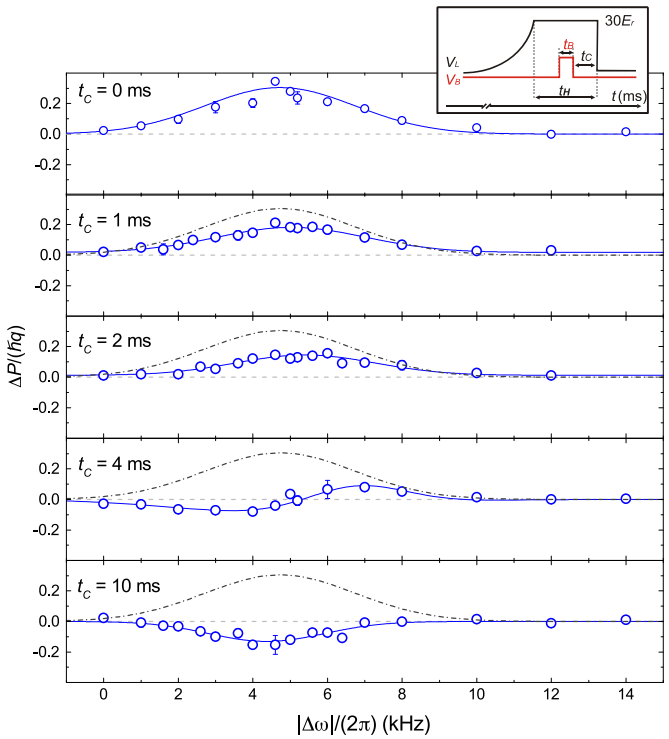

Figure 5. In-trap dynamics after the Bragg excitation. $\Delta P/(\hbar q)$ is reported as a function of $|\Delta\omega|/(2\pi)$, for different holding times in the trap after the Bragg excitation: $t_C = 0,\ 1,\ 2,\ 4,\ 10$ ms. The continuous blue lines are guides for the eyes. The curve corresponding to $t_C = 0$ ms is also reported in the other panels (as a dashed-dotted line) for comparing the signal shapes and amplitudes. Inset: experimental time sequence. The total holding time in the lattices is kept constant ($t_H = 30$ ms).

in-trap dynamics before the release [20, 33]. For the cases discussed so far (see figures 2 and 3), the momentum transferred has been measured immediately after the Bragg pulse. for the 1D gases, even if $t_B \simeq T/5$, as seen in section 2.2, ΔP and ΔE—which is not affected by in-trap dynamics since energy is a conserved quantity—carry the same information. Thus, we cannot infer appreciable effects of the dynamics during the Bragg pulse in the momentum spectrum recorded immediately after the Bragg pulse.

Now, we characterize more in depth the effect of the in-trap dynamics on the response of the 1D gases. To this purpose, we measure $\Delta P\,(q,\ \omega)/(\hbar q)$ at variable time after the end of the Bragg perturbation. In figure 5(a) we can observe a modification of the system response with time. The Bragg time-duration is fixed to the value $t_B = 3$ ms, and the total holding-time of the atoms in the lattice trap (t_H) is kept constant, while we vary the time t_C between the end of the Bragg pulse and the release of the trap from 0 ms up to 10 ms, as sketched in the inset of the figure. During the first 2 ms after the Bragg pulse, the total spectral weight of the signal undergoes a suppression with time (note that the vertical scale is the same in all the panels of the figure), which eventually results in a negative amplitude at $t_C = 10$ ms. Remarkably, the shape of the signal at $t_C = 4$ ms is asymmetric and qualitatively different from the other cases.

The latter behavior can be qualitatively interpreted by considering the effect of the in-trap dynamics *during* the Bragg pulse. Let us consider a system of N interacting particles trapped in a harmonic potential, described by the following Hamiltonian

$$H = \sum_{i=1}^{N}\left[\frac{\hat{\boldsymbol{p}}_i^{\,2}}{2m} + V_{\rm ho}(\boldsymbol{x}_i) + \sum_{j<i} V^{\rm int}(\boldsymbol{x}_i - \boldsymbol{x}_j)\right]. \tag{4}$$

The evolution of the total momentum and position operators along each spatial directions can be easily obtained from the Heisenberg equations as $\dot{\hat{p}}_\alpha = (-i/\hbar)[\hat{H},\ \hat{p}_\alpha] = m\omega^2\hat{x}_\alpha$ and $\dot{\hat{x}}_\alpha = (-i/\hbar)[\hat{H},\ \hat{x}_\alpha] = -\hat{p}_\alpha/m$, with $\hat{O}_\alpha = \sum_{i=1}^{N}\hat{O}_{i\alpha}$ ($\alpha = 1,\ 2,\ 3$, $\hat{\boldsymbol{O}} = \hat{\boldsymbol{x}},\ \hat{\boldsymbol{p}}$). For the first relation we have used the fact that $\partial_{x_{j\alpha}} V_{ij}^{\rm int} = -\partial_{x_{i\alpha}} V_{ij}^{\rm int}$. Then, restricting the discussion to the 1D case, it is straightforward to get that the average momentum evolves in the trap as

$$\langle p\rangle(t) = -m\omega_x\langle\hat{x}\rangle_0\sin(\omega_x t) + m\langle\dot{\hat{x}}\rangle_0\cos(\omega_x t), \tag{5}$$

where $\langle\hat{x}\rangle_0$ and $\langle\dot{\hat{x}}\rangle_0$ are the average position (center-of-mass) and velocity at time $t = 0^+$ immediately after the end of the Bragg pulse. We remark that this result is valid in general for any interacting system, regardless of the

temperature, the statistics (being the particles bosons or fermions) and the dimensionality of the system. In fact, it is a well known result that the dynamics of the center of mass in the presence of harmonic trapping is decoupled from the internal degrees of freedom of the system (see e.g. [17]).

Let us now turn to the effect of the Bragg pulse, that we assume of the form $g(t)\,V_B\cos(qx-\omega t)$. First, let us consider the case of a Bragg pulse duration $t_B \ll T$, which can be considered as *instantaneous* with respect to the in-trap dynamics. After the pulse, at $t = 0^+$, the density distribution is basically unperturbed ($\langle\hat{x}\rangle_0 = 0$). Then, the Bragg perturbation only affects the initial velocity distribution $n(\hat{x}_0)$, so that its mean value is $\langle\hat{x}\rangle_0 = (N_B/N)\,\hbar q/m$, where N_B/N is the ratio of the number of diffracted atoms to the total number of atoms. As follows from equation (5), in this case $\langle p\rangle(t)$ vanishes exactly for $t = T/4$, T being the period of the trap, for any excitation frequency.

Instead, for a finite duration of the Bragg pulse (and in particular, if t_B is comparable with the trap period), even the spatial distribution of the atomic ensemble may undergo modifications during the Bragg perturbation, depending on the excitation frequency. This makes the initial value of the center-of-mass $\langle\hat{x}\rangle_0$ in equation (5) non vanishing and ω-dependent, therefore affecting the following dynamics and changing the shape of the signal.

As an example, let us consider the simple case of a Bose–Einstein condensate in a *single*, quasi 1D tube, in the mean-field regime. In this case, the response of the system to the Bragg pulse can be easily obtained by solving the following 1D Gross–Pitaevskii equation ($t \geqslant 0$):

$$i\hbar\partial_t\psi = \left[-\frac{1}{2m}\nabla_x^2 + V_{\rm ho}(x) + \theta(t-t_B)\,V_B\cos(qx-\omega t) + g_{1D}\,|\psi|^2\right]\psi, \tag{6}$$

where $g_{1D} = g/(2\pi a_\perp)$, $g = 4\pi\hbar^2 a/m$ being the 3D interaction strength, a the scattering length for ^{87}Rb, and $a_\perp = \sqrt{\hbar/(m\omega_\perp)}$ the oscillator length in the transverse directions. In this specific example we consider $V_B/h = 120$ Hz, $t_B = 3$ ms, $\omega_x = 2\pi\times 60$ Hz, $\omega_\perp = 2\pi\times 42$ kHz, and an array of tubes that corresponds to the typical experimental configuration. The response of the system at different evolution times in the trap is shown in figure 6, where the meanfield predictions are also compared to the non-interacting case[7]. This figure shows that indeed, as follows from equation (5), the response pattern at $t = T/2$ is reversed with respect to that at $t = 0$, the evolution being periodic in time. For intermediate times, the shape of the signal is non trivial, depending on the relative weight and on the specific shape of the transferred momentum and the center of mass position as a function of the Bragg frequency $|\Delta\omega|$, at $t = 0$. In the non interacting case, $\langle p\rangle_0(|\Delta\omega|)$ and $\langle x\rangle_0(|\Delta\omega|)$ are centered at the same value and almost symmetric around that point, so that the same symmetry property is preserved during the evolution. Instead, the response of an interacting condensate is characterized by a distribution of the center-of-mass position that is peaked at higher frequency with respect to the corresponding transferred momentum, and this affects dramatically the shape at intermediate times. In particular, at $t \simeq 0.15T$ the signal shape has a characteristic sinusoidal-like form, whereas at $t = 0.25T$ it corresponds exactly to the reverse of the initial center-of-mass distribution $\langle x\rangle_0(|\Delta\omega|)$. Note that the signal at $t \simeq 0.15T$ is analogous to that observed experimentally at $t = 4$ ms, see figure 5, though in that case the signal first reverses in the low frequency region. In fact, as discussed above, according to equation 5 the specific shape of the response function depends on the form and on the relative position (as a function of $|\Delta\omega|$) of $\langle\hat{x}\rangle_0$ and $\langle\hat{x}\rangle_0$ immediately after the end of the Bragg pulse. Notice that a small displacement between the two distributions is sufficient to reverse the shape of the signal observed at $t \simeq 0.15T$ in figure 6(b). Therefore, as the response of the system to the Bragg perturbation in the strong-coupling regime is expected to be substantially different with respect to the mean field case[8], it is not surprising that the shape of the signal at $t = 4$ ms in figure 5 turns out to be reversed.

4. Conclusions

In conclusion, we have investigated the response of an array of 1D gases, comparing energy and momentum transfer in Bragg spectroscopy experiments. In the presence of an external trapping potential along the axis of the tubes, even if increasing the pulse time enhances the spectral resolution, the presence of the trap in principle provides an upper limit to the pulse duration. Our experiment reveals that, in a regime of parameters well described by the linear response theory, and for time-duration of the Bragg perturbation smaller than a quarter of the trapping period, the proportionality relation between the momentum transfer and the dynamic structure factor is well respected. We also show that the in-trap dynamics during the Bragg pulse affects noticeably the response of the system. Since the in-trap dynamics could be affected by the regime of interaction of the system, one may consider to use the momentum as a probe of the emergence of the strongly correlated regime. The

[7] The value of the amplitude V_B/h of the Bragg pulse in the simulations is chosen in order to lie in the linear response regime for the non-interacting case with a pulse length of $t_B = 3$ ms.

[8] We remark that a precise simulation of the dynamics of strongly correlated 1D systems under the effect of a Bragg perturbation can be very demanding, see e.g. [35], and goes beyond the scope of this work.

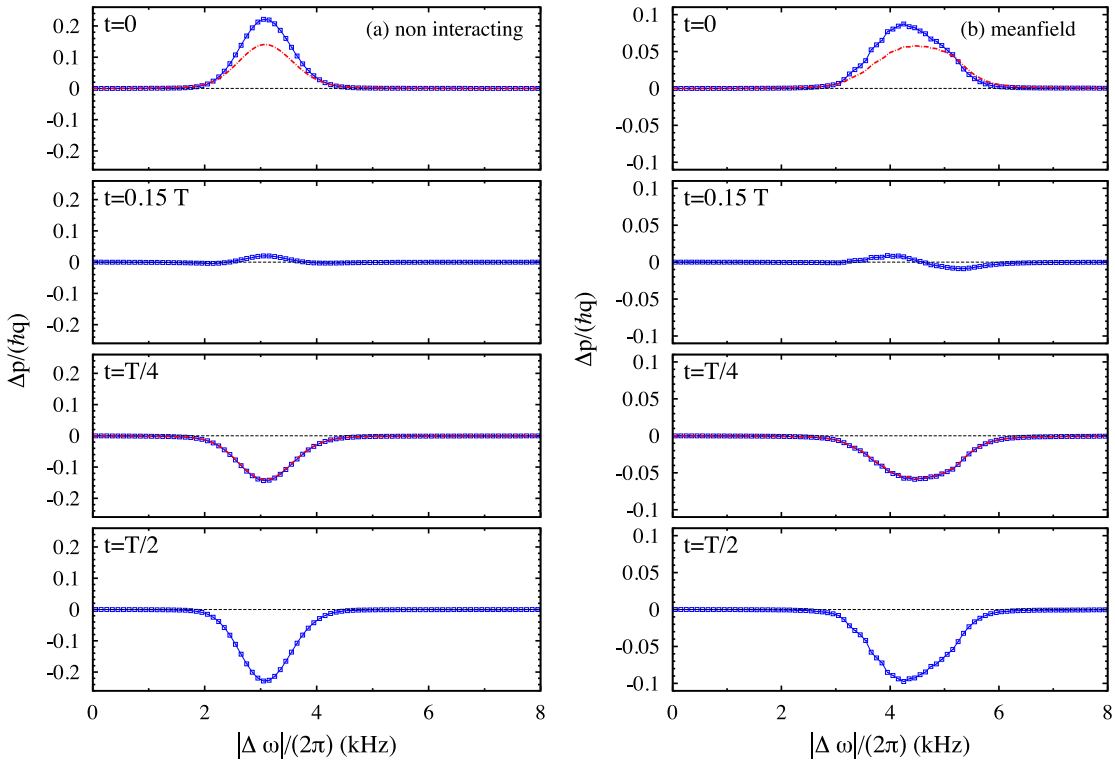

Figure 6. In-trap dynamics of a condensate in the mean field regime. Theoretical prediction for the value of $\Delta P/(\hbar q)$ (blue squares) as a function of the Bragg frequency for an array of quasi 1D BECs, for different holding times in the trap after the Bragg excitation: $t = 0,\ 0.15,\ 0.25,\ 0.5T$ (T being the trap period). The dotted-dashed (red) lines in the top panel represent the initial distributions of the center-of-mass $\langle x\rangle_0$ ($|\Delta\omega|$). The same line is shown inverted at $t = T/4$ (see text). The left and right columns correspond to (a) the non interacting and (b) interacting case in the mean-field regime, respectively.

analysis performed in this work can be useful for interpreting the results of scattering experiments also in other more complex settings of ultracold gases in optical lattices or disordered potentials, and can be also relevant for further techniques such as lattice amplitude modulation [12] and photo-emission spectroscopy [36] in ultracold gases experiments.

Acknowledgments

The authors would like to acknowledge the BEC1 apparatus for its fifteen years of work and all the people—students, technicians, and researchers—who have contributed to this exciting period. We would like to acknowledge L Fallani for critical reading of the manuscript. This work has been supported by ERC through the Advanced Grant DISQUA (Grant 247371), and by EC through EU FP7 the Integrated Project SIQS (Grant 600645), Universidad del Pais Vasco/Euskal Herriko Unibertsitatea under Programs No. UFI 11/55, Ministerio de Economía y Competitividad through Grant No. FIS2012-36673-C03-03, and the Basque Government through Grant No. IT-472-10.

References

[1] Wollan E O 1932 *Rev. Mod. Phys.* **4** 205
[2] Bramwell S T and Keimer B 2014 *Nat. Mater.* **13** 763–7
[3] Stenger J, Inouye S, Chikkatur A P, Stamper-Kurn D M, Pritchard D E and Ketterle W 1999 *Phys. Rev. Lett.* **82** 4569
[4] Kozuma M, Deng L, Hagley E W, Wen J, Lutwak R, Helmerson K, Rolston S L and Phillips W D 1999 *Phys. Rev. Lett.* **82** 871
[5] Steinhauer J, Ozeri R, Katz N and Davidson N 2002 *Phys. Rev. Lett.* **88** 120407
[6] Richard S, Gerbier F, Thywissen J H, Hugbart M, Bouyer P and Aspect A 2003 *Phys. Rev. Lett.* **91** 010405
[7] Ernst P T, Götze S, Krauser J S, Pyka K, Lühmann D-S, Pfannkuche D and Sengstock K 2010 *Nat. Phys.* **6** 56
[8] Bissbort U *et al* 2011 *Phys. Rev. Lett.* **106** 205302
[9] Papp S B, Pino J M, Wild R J, Ronen S, Wieman C E, Jin D S and Cornell E A 2008 *Phys. Rev. Lett.* **101** 135301
[10] Veeravalli G, Kuhnle E, Dyke P and Vale C J 2008 *Phys. Rev. Lett.* **101** 250403
[11] Pagano G *et al* 2014 *Nat. Phys.* **10** 198
[12] Stöferle T, Moritz H, Schori C, Kohl M and Esslinger T 2004 *Phys. Rev. Lett.* **92** 130403
[13] Clément D, Fabbri N, Fallani L, Fort C and Inguscio M 2009 *Phys. Rev. Lett.* **102** 155301

[14] Fabbri N, Huber S D, Clément D, Fallani L, Fort C, Inguscio M and Altman E 2012 *Phys. Rev. Lett.* **109** 055301
[15] Fabbri N, Clément D, Fallani L, Fort C and Inguscio M 2011 *Phys. Rev.* A **83** 031604(R)
[16] Fabbri N, Panfil M, Clément D, Fallani L, Inguscio M, Fort C and Caux J-S 2014 *Phys. Rev.* A **91** 043617
[17] Dalfovo F, Giorgini S, Pitaevskii L P and Stringari S 1999 *Rev. Mod. Phys.* **71** 463
[18] Sherson J F, Weitenberg C, Endres M, Cheneau M, Bloch I and Kuhr S 2010 *Nature* **467** 68
[19] Brunello A, Dalfovo F, Pitaevskii L, Stringari S and Zambelli F 2001 *Phys. Rev.* A **64** 063614
[20] Blakie P B, Ballagh R J and Gardiner C W 2002 *Phys. Rev.* A **65** 033602
[21] Paredes B, Widera A, Murg V, Mandel O, Fölling S, Cirac J I, Shlyapnikov G V, Haensch T W and Bloch I 2004 *Nature* **429** 277
[22] Kinoshita T, Wenger T and Weiss D 2004 *Science* **305** 1125
[23] Haller E, Hart R, Mark M J, Danzl J G, Reichsöllner L, Gustavsson M, Dalmonte M, Pupillo G and Nägerl H-C 2009 *Science* **325** 1224
[24] Giamarchi T 2004 *Quantum Physics in One Dimension* (Oxford: Oxford University Press)
[25] Kinoshita T, Wenger T and Weiss D S 2006 *Nature* **440** 900
[26] Langen T, Geiger R, Kuhnert M, Rauer B and Schmiedmayer J 2013 *Nat. Phys.* **9** 640
[27] Kheruntsyan K V, Gangardt D M, Drummond P D and Shlyapnikov G V 2005 *Phys. Rev.* A **71** 053615
[28] Greiner M, Mandel O, Esslinger T, Hänsch T W and Bloch I 2002 *Nature* **415** 39
[29] Olshanii M 1998 *Phys. Rev. Lett.* **81** 938
[30] Stringari S and Pitaevskii L P 2003 *Bose–Einstein Condensation* (Oxford: Clarendon)
[31] Zambelli F, Pitaevskii L, Stamper-Kurn D M and Stringari S 2000 *Phys. Rev.* A **61** 063608
[32] Katz N, Ozeri R, Steinhauer J, Davidson N, Tozzo C and Dalfovo F 2004 *Phys. Rev. Lett.* **93** 220403
[33] Tozzo C and Dalfovo F 2003 *New. J. Phys.* **5** 54
[34] The time-dependent Schrödinger and Gross–Pitaevskii equations are solved by means of a FFT split-step method, see e.g. Jackson B, McCann J F, Adams C S1998 *J. Phys. B: At. Mol. Opt. Phys.* **31** 4489
[35] Cazalilla M, Citro R, Giamarchi T, Orignac E and Rigol M 2011 *Rev. Mod. Phys.* **83** 1405
[36] Stewart J T, Gaebler J P and Jin D S 2008 *Nature* **454** 744